

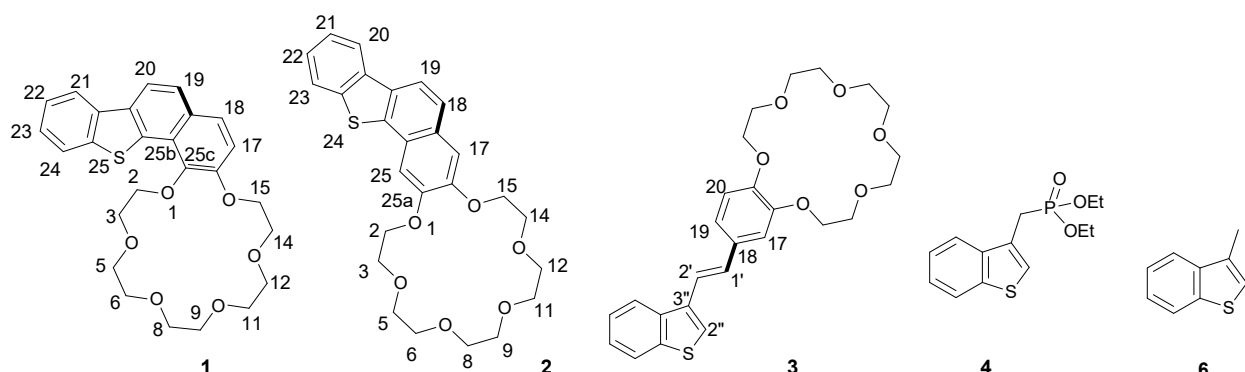
## Supplementary info

# Congestion effect of an annulated tetracyclic thiophene-containing fragment on 18-crown-6 ether: manifestation in complex formation in solution and membrane transfer properties

Andrey Khoroshutin<sup>a</sup>, Leonid Martynov<sup>b</sup>, Polina Yaltseva<sup>a</sup> †, Evita Kostenko<sup>b</sup>, Dmitry Cheshkov<sup>b</sup>, Anatoliy Botezatu<sup>c</sup>, Anna Moiseeva<sup>a</sup>, Yuri Fedorov<sup>c</sup> and Olga Fedorova<sup>c</sup>

## CONTENTS

1. NMR spectra.....	1
2. 2D spectra .....	4
3. High-resolution mass-spectrometry of <u>1</u> and <u>2</u> .....	7
4. Titrations.....	9
4.1. NMR titration .....	9
4.2. UV-Vis and fluorescence titration .....	13
5. DOSY experiments on native and complexed CE <u>1</u> and CE <u>2</u> .....	14
6. Representative conformations of crown ethers <u>1</u> and <u>2</u> .....	15
6.1. Generating conformations with dihedral angles close to 0 Deg .....	15
6.2. Docking of the aromatic fragment and MMF94 optimization both in vacuo and in CH <sub>3</sub> CN ( $\epsilon = 38.8$ ).....	19
6.3. Single point energy and NMR chemical shifts calculations .....	20
7. Facilitated ion transfer measurements .....	24



## 1.NMR spectra

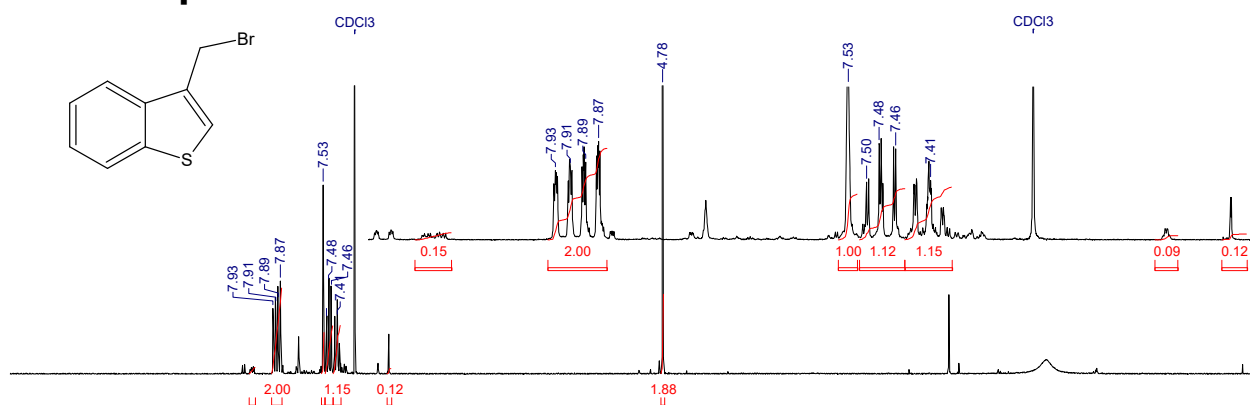
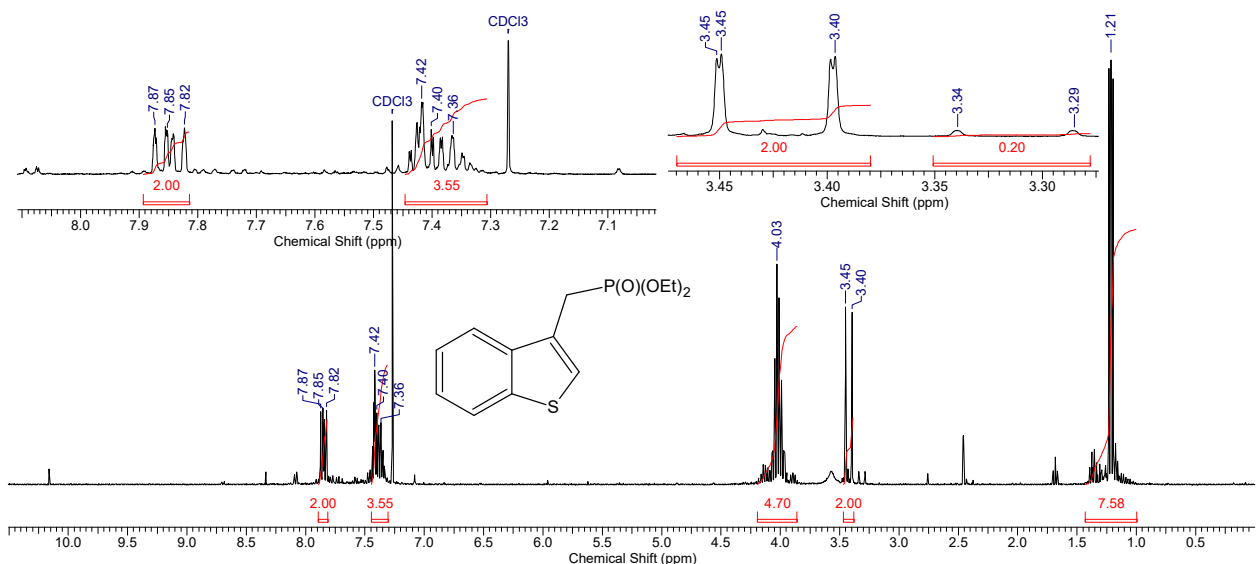
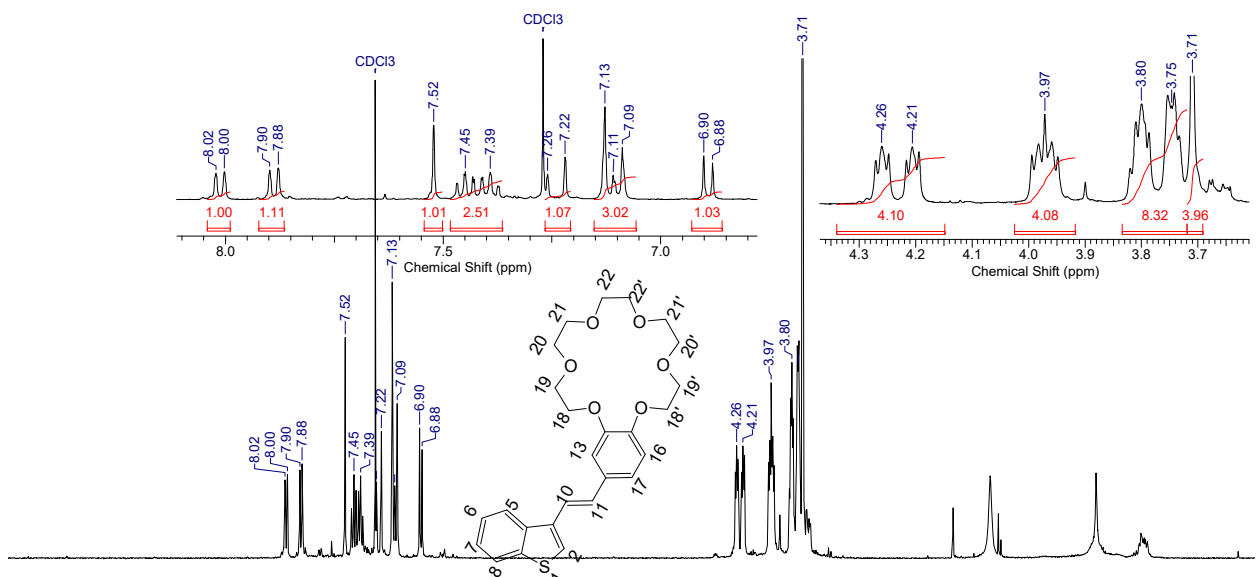


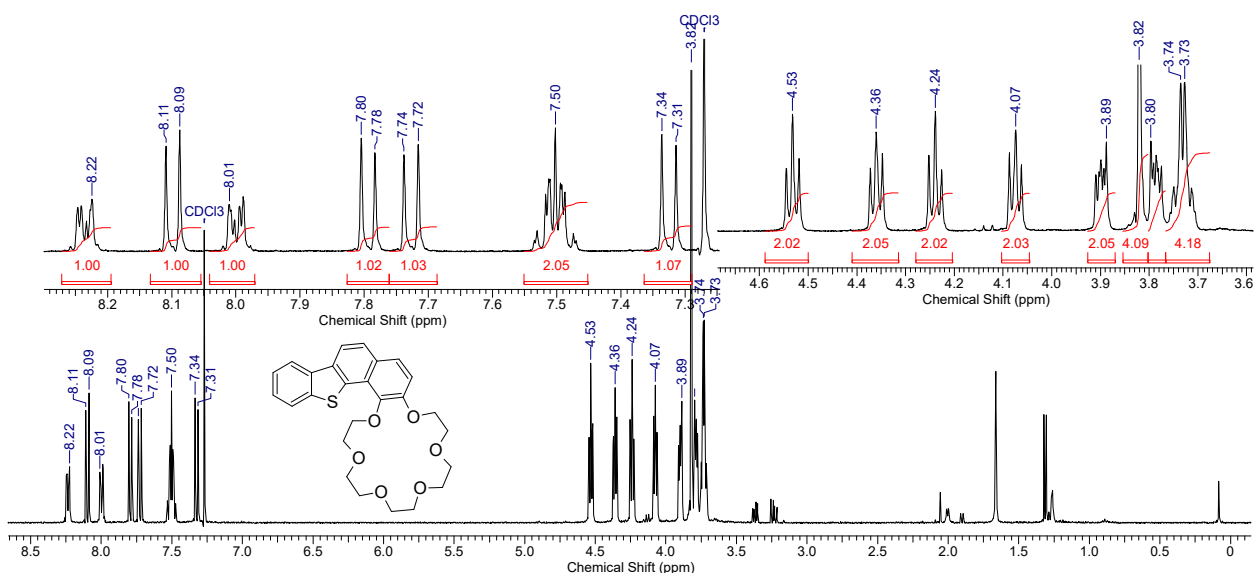
Figure S1. <sup>1</sup>H NMR spectrum (400 MHz, CDCl<sub>3</sub>) of 3-bromomethylbenzothiophene.



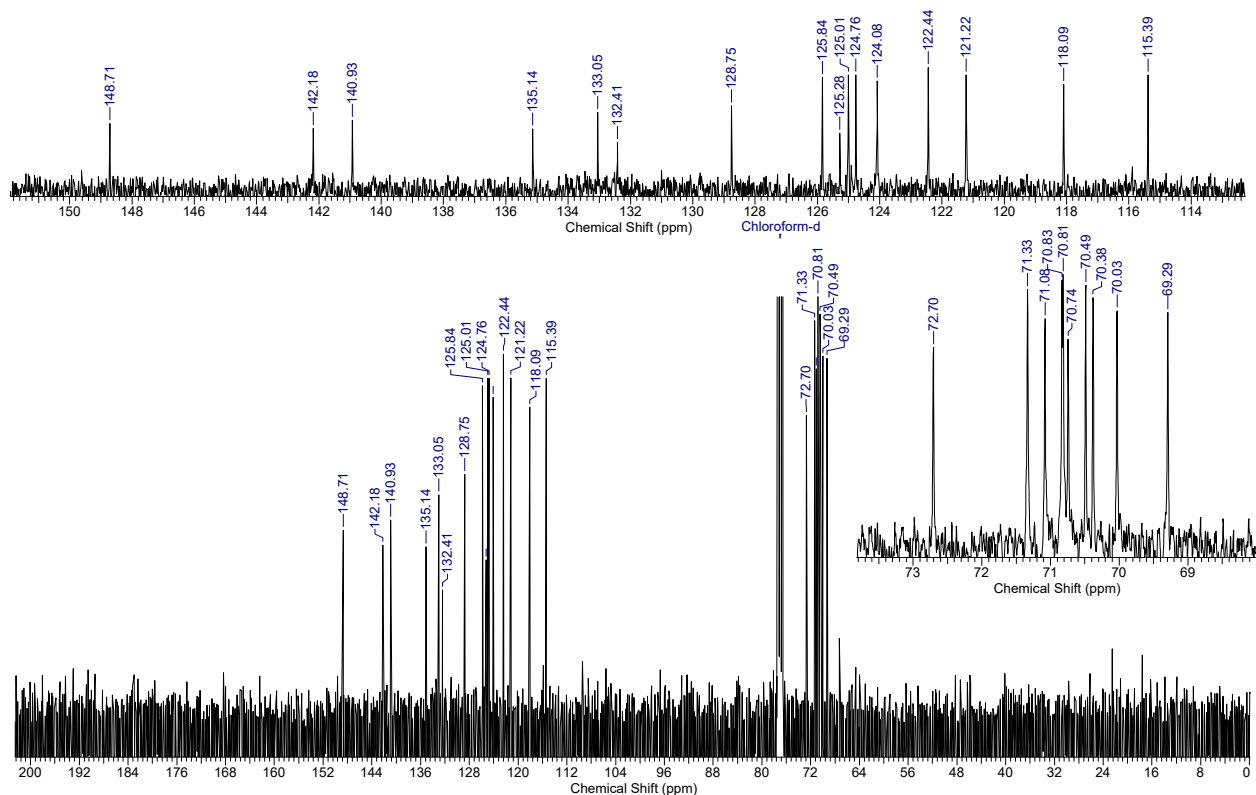
**Figure S2.**  $^1\text{H}$  NMR spectrum (400 MHz,  $\text{CDCl}_3$ ) of **4**.



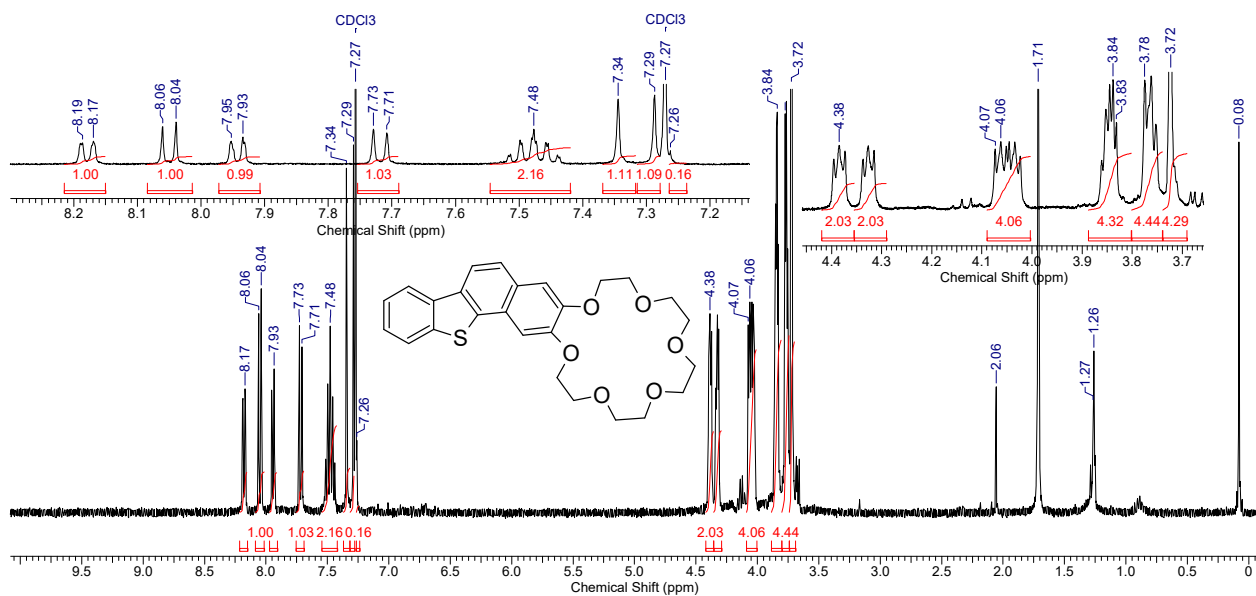
**Figure S3.**  $^1\text{H}$  NMR spectrum (400 MHz,  $\text{CDCl}_3$ ) of **3**.



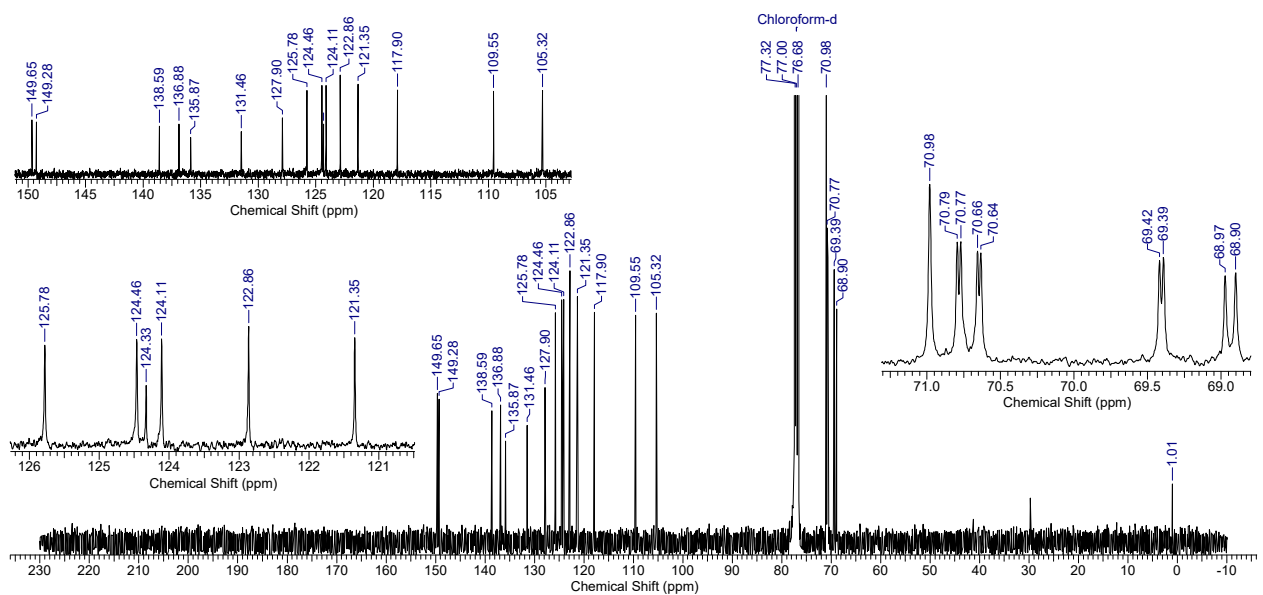
**Figure S4.**  $^1\text{H}$  NMR spectrum (400 MHz,  $\text{CDCl}_3$ ) of **1**.



**Figure S5.**  $^{13}\text{C}$  NMR spectrum (400 MHz,  $\text{CDCl}_3$ ) of **1**.

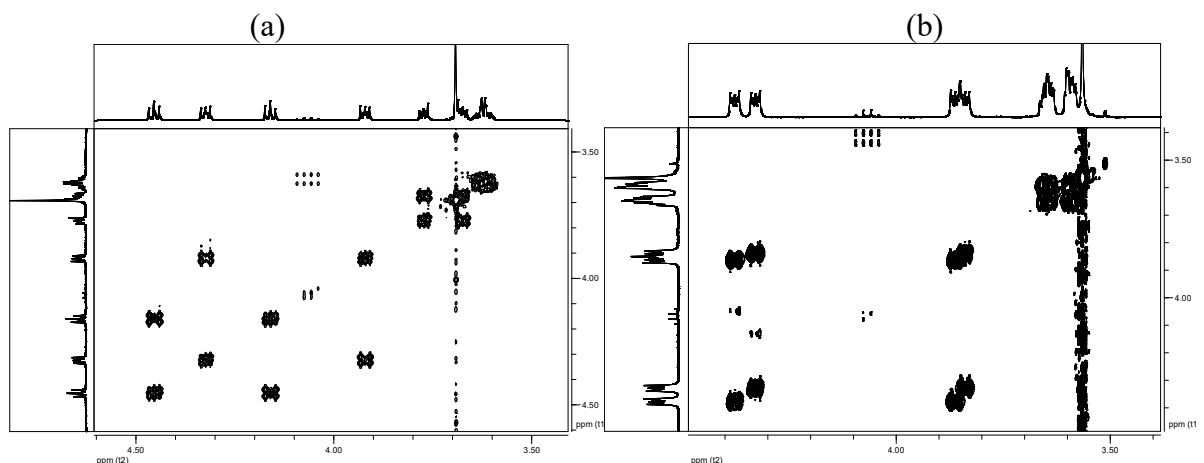


**Figure S6.**  $^1\text{H}$  NMR spectrum (400 MHz,  $\text{CDCl}_3$ ) of **2**.

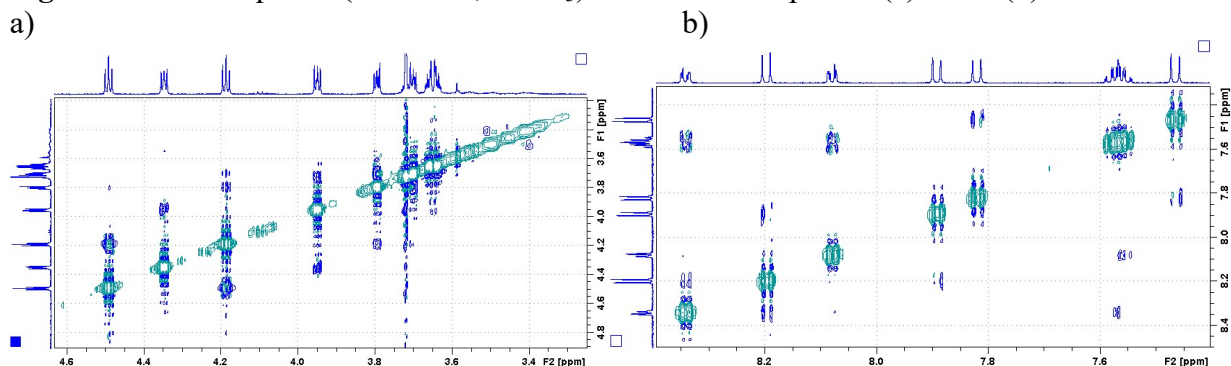


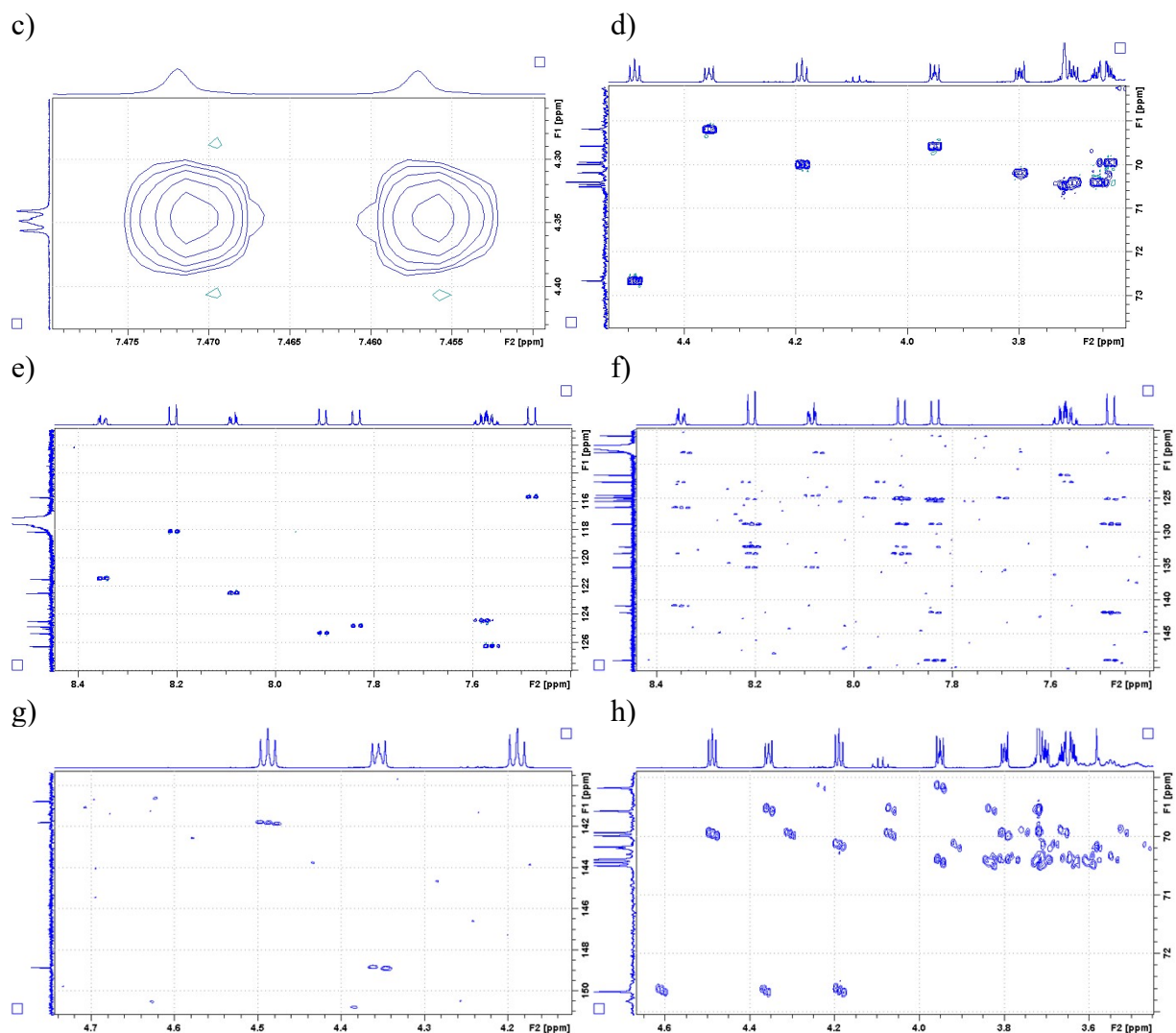
**Figure S7.** <sup>13</sup>C NMR spectrum (400 MHz, CDCl<sub>3</sub>) of **2**.

## 2. 2D spectra

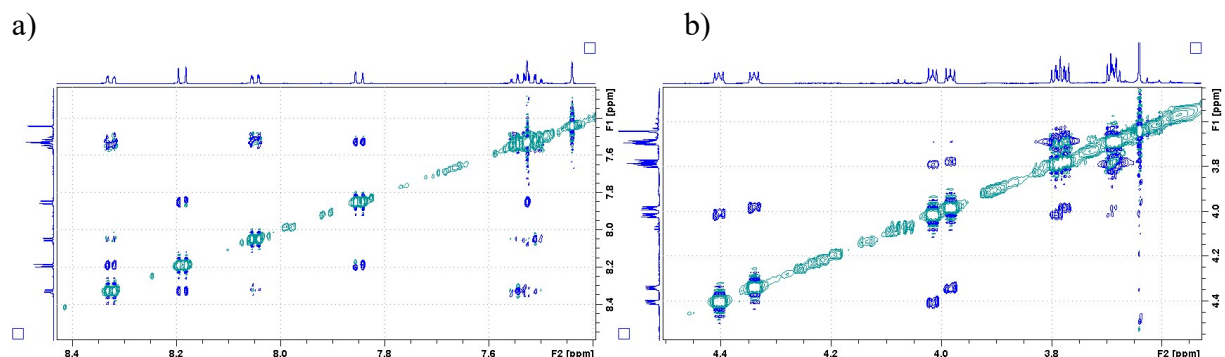


**Figure S8** COSY spectra (400 MHz, CDCl<sub>3</sub>) of crown ether part of (a) **1** and (b) **2**.





**Figure S9.** NOESY; HMBS, HSQC of **1** (600 MHz,  $\text{CD}_3\text{CN}$ ). a) NOESY of the crown ether part; b) NOESY of the aromatic part; c) NOESY cross-peak between aromatic and crown ether part; d) HSQC of the aromatic part; e) HSQC of the crown ether part; f) HMBC of the aromatic region; g) HMBC cross peaks between crown ether and aromatic part; h) HMBC of the aromatic part.



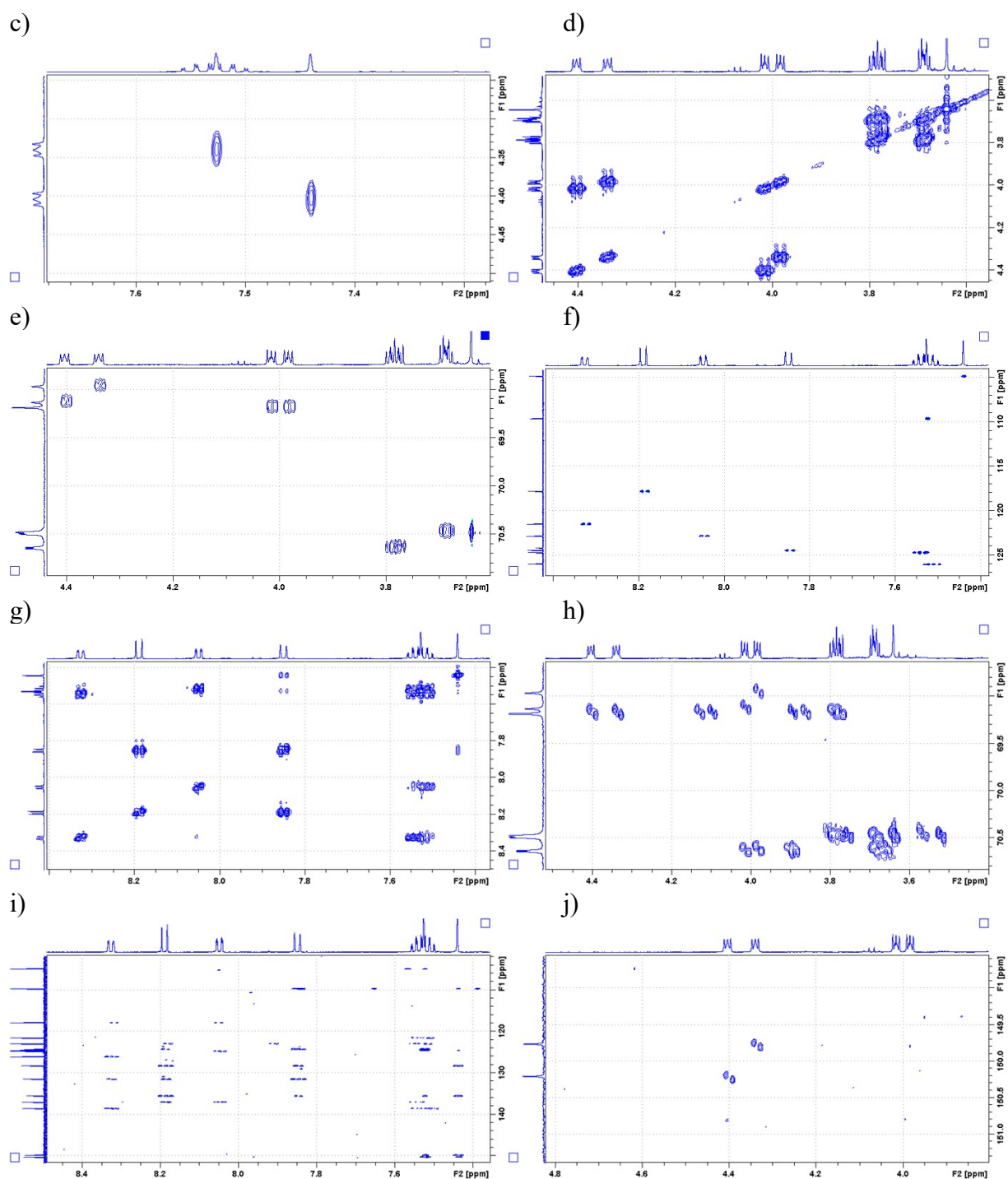


**Figure S10.** NOESY; HMBS, HSQC of **2** (600 MHz,  $\text{CD}_3\text{CN}$ ). a) NOESY of the aromatic part; b) NOESY of the crown ether part; c) NOESY cross-peaks between aromatic and crown ether part; d) COSY of the crown ether part; e) COSY of the aromatic part; f) HSQC of the crown ether region; g) HSQC of aromatic region; h) HMBC of the crown part; i) HMBC of the aromatic region; j) HMBC cross peaks between crown ether and aromatic part.

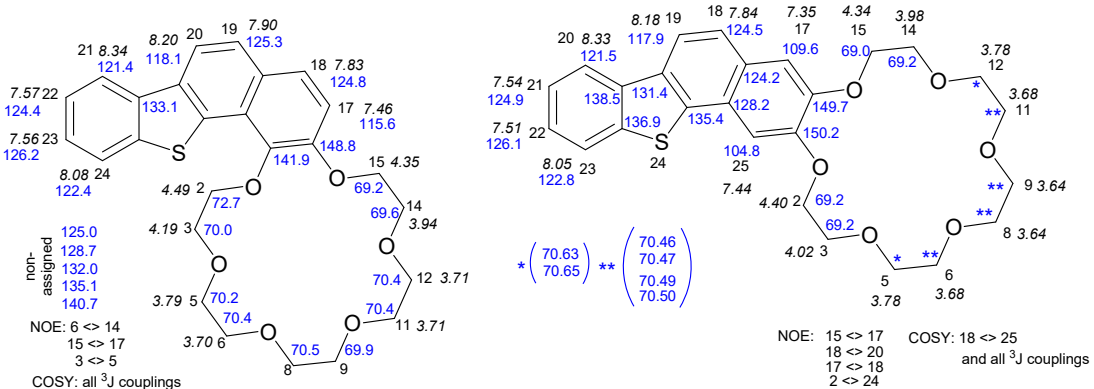
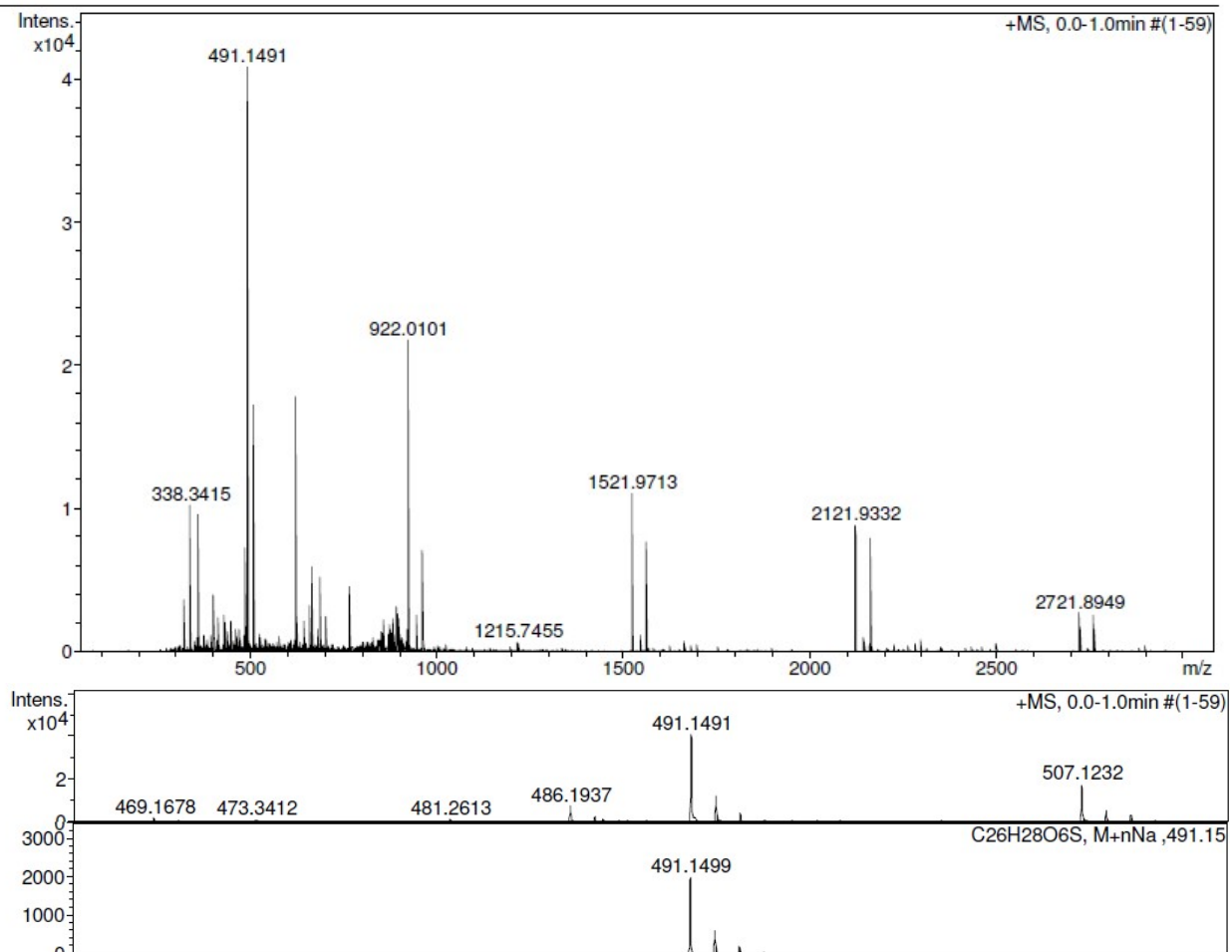


**Figure S11.** NMR assignments ( $^1\text{H}$  shown in italic,  $^{13}\text{C}$  shown in blue) based on NOESY; HMBS, HSQC of **1** ( $\text{CD}_3\text{CN}$ ) and **2** ( $(\text{CD}_3)_2\text{CO}$ ) (600 MHz).

### 3. High-resolution mass-spectrometry of **1** and **2**.

#### Acquisition Parameter

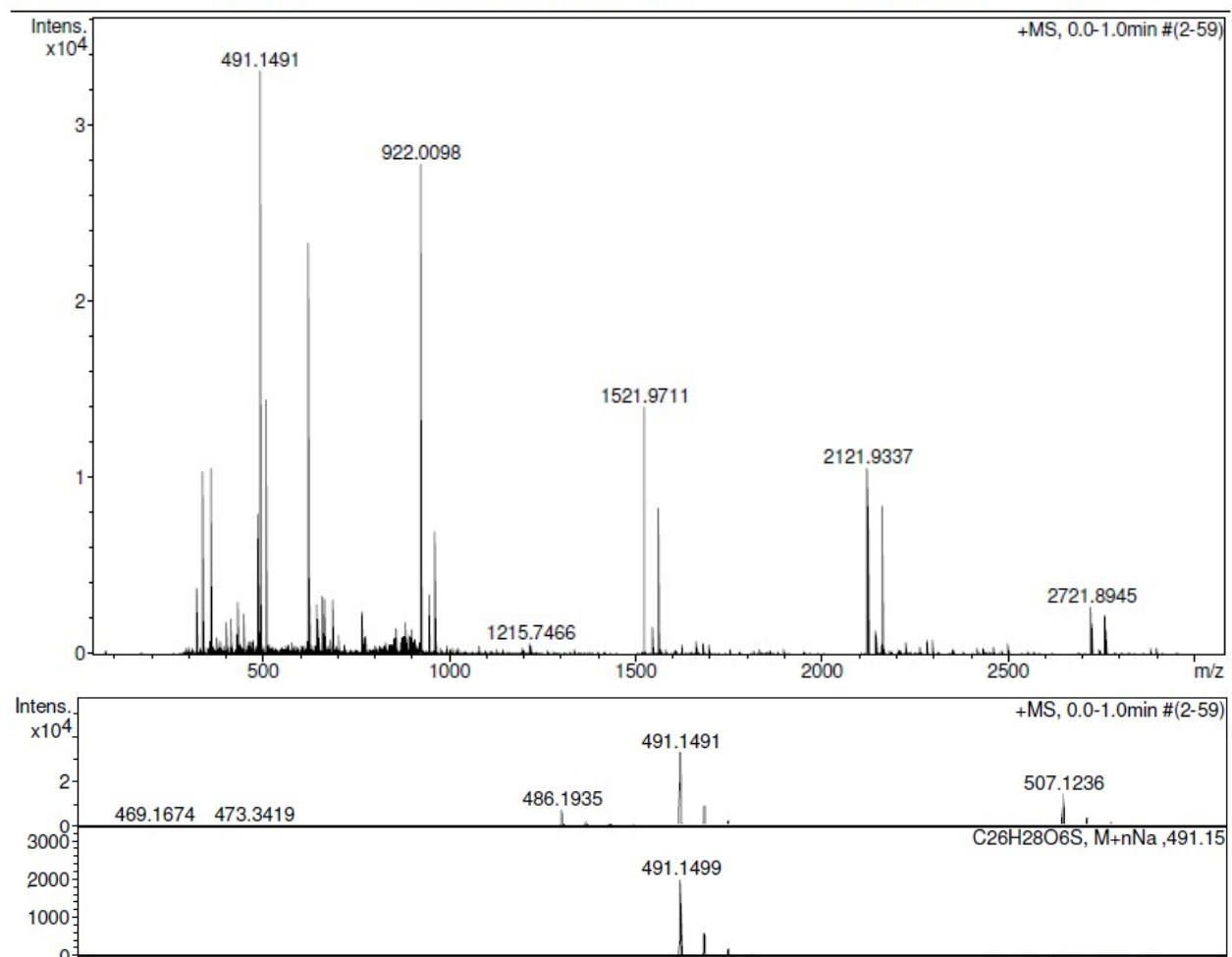
Source Type	ESI	Ion Polarity	Positive	Set Nebulizer	0.4 Bar
Focus	Not active			Set Dry Heater	180 °C
Scan Begin	50 m/z	Set Capillary	4500 V	Set Dry Gas	4.0 l/min
Scan End	3000 m/z	Set End Plate Offset	-500 V	Set Divert Valve	Waste



**Figure S12.** HRMS of **1**.

**Acquisition Parameter**

Source Type	ESI	Ion Polarity	Positive	Set Nebulizer	0.4 Bar
Focus	Not active			Set Dry Heater	180 °C
Scan Begin	50 m/z	Set Capillary	4500 V	Set Dry Gas	4.0 l/min
Scan End	3000 m/z	Set End Plate Offset	-500 V	Set Divert Valve	Waste

**Figure S13.** HRMS of **2**.

## 4.Titrations

### 4.1. NMR titration

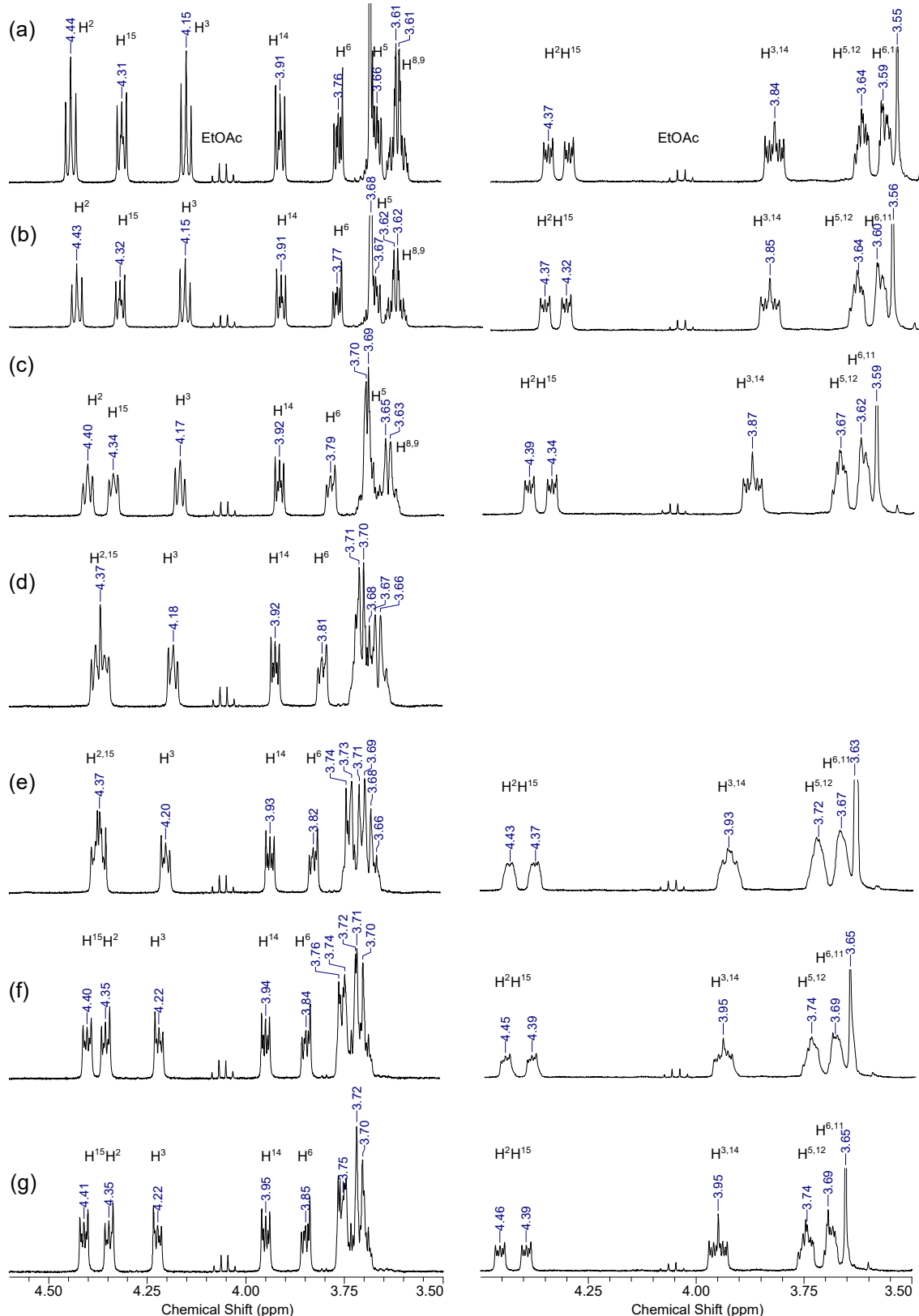


**Figure S14** NMR titration (400 MHz,  $\text{CD}_3\text{CN}$ ) results of **1** (left) and **2** (right) by  $\text{NH}_4\text{ClO}_4$  (crown ether part of the spectrum). Salt to crown ether ratio: (a) – 0; (b) – 0.1; (c) – 0.3; (d) – 0.5; (e) – 0.7; (f) – 1; (g) - excess.

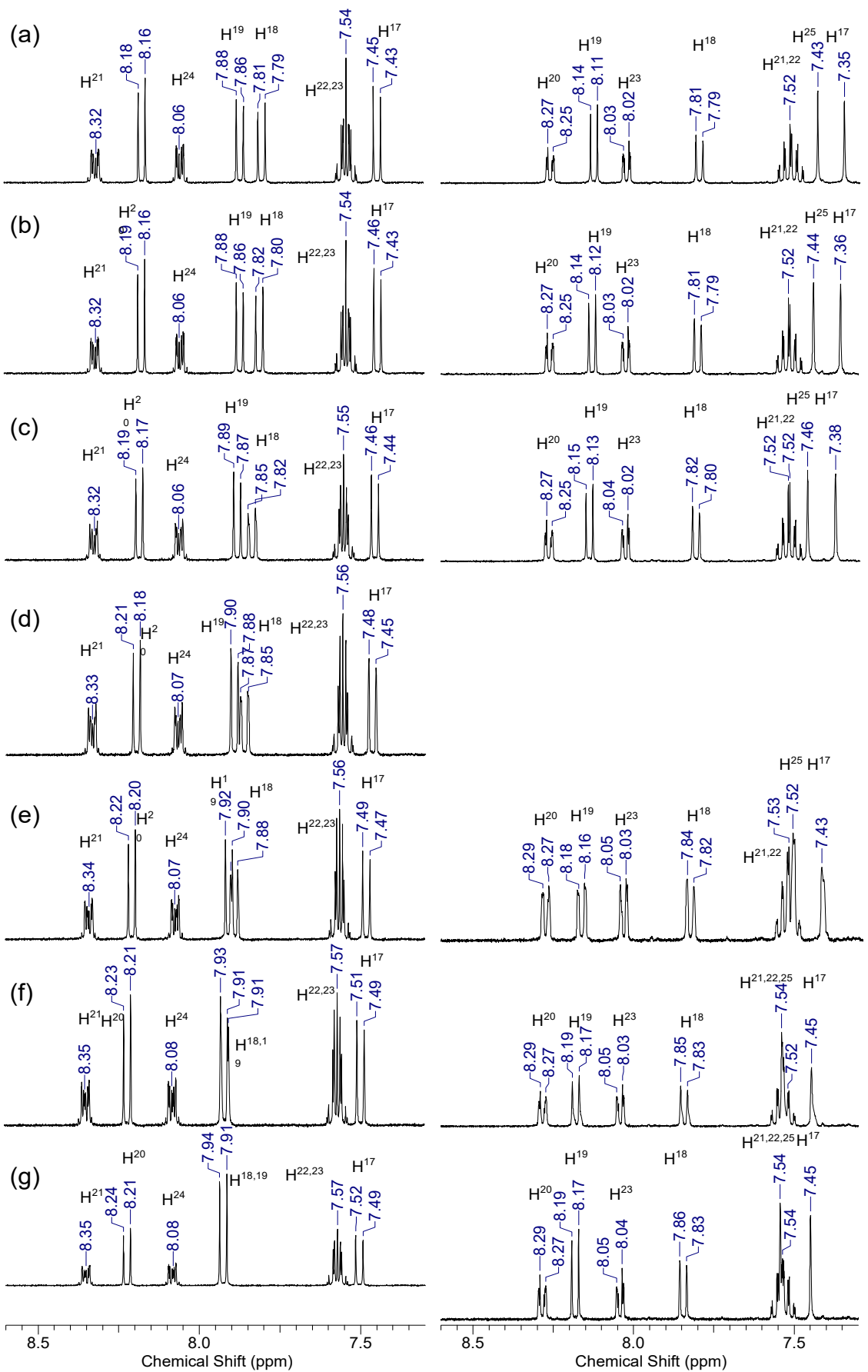


**Figure S15** NMR titration (400 MHz, CD<sub>3</sub>CN) results of **1** (left) and **2** (right) by NH<sub>4</sub>ClO<sub>4</sub> (aromatic part of the spectrum). Salt to crown ether ratio: (a) – 0; (b) – 0.1; (c) – 0.3; (d) – 0.5; (e) – 0.7; (f) – 1; (g) - excess.

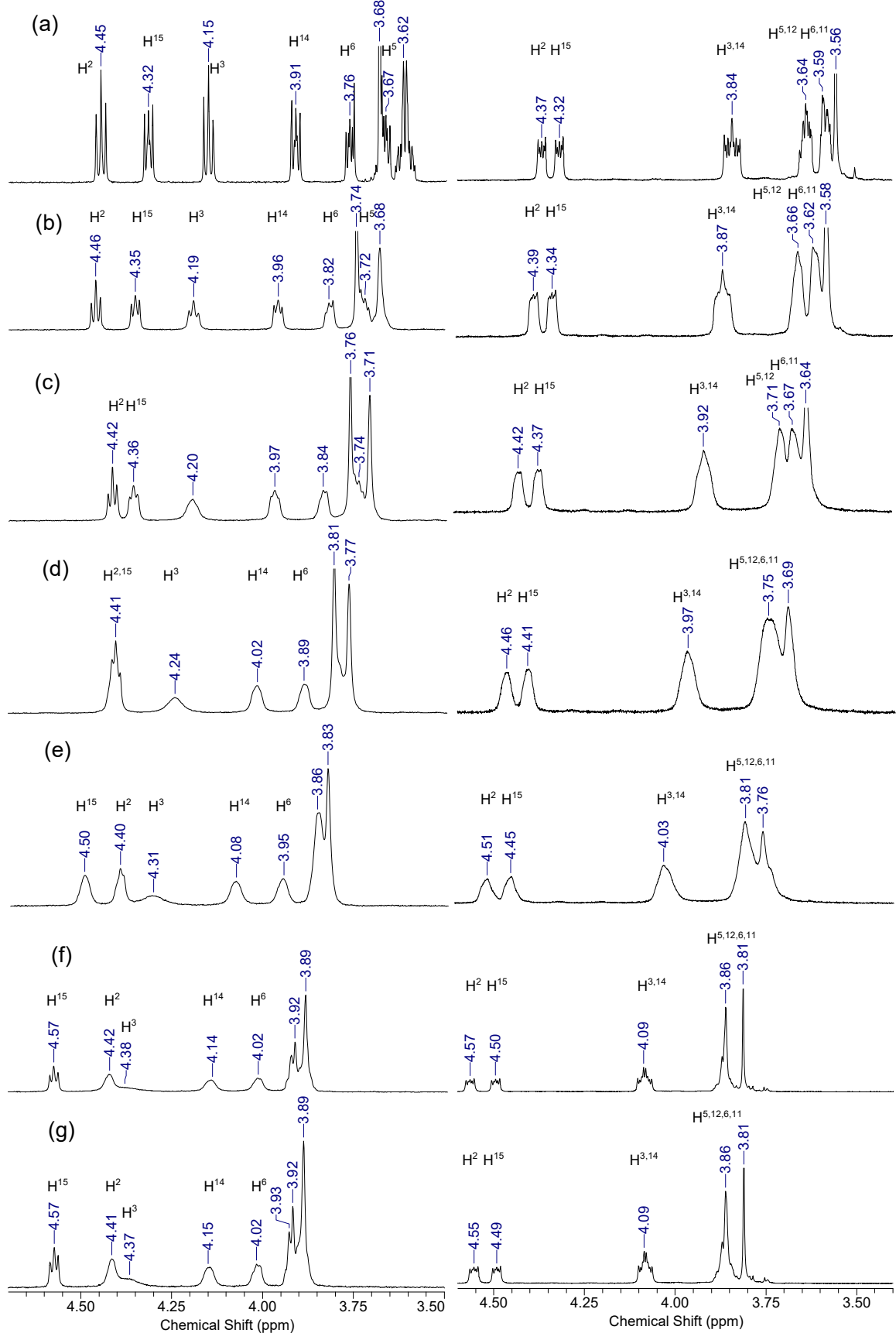


**Figure S16** NMR titration (400 MHz, CD<sub>3</sub>CN) results of **1** (left) and **2** (right) Ba(ClO<sub>4</sub>)<sub>2</sub> (crown ether part). Salt to crown ether ratio: (a) - 0; (b) - 0.1; (c) - 0.3; (d) - 0.5; (e) - 0.7; (f) - 1; (g) - excess.

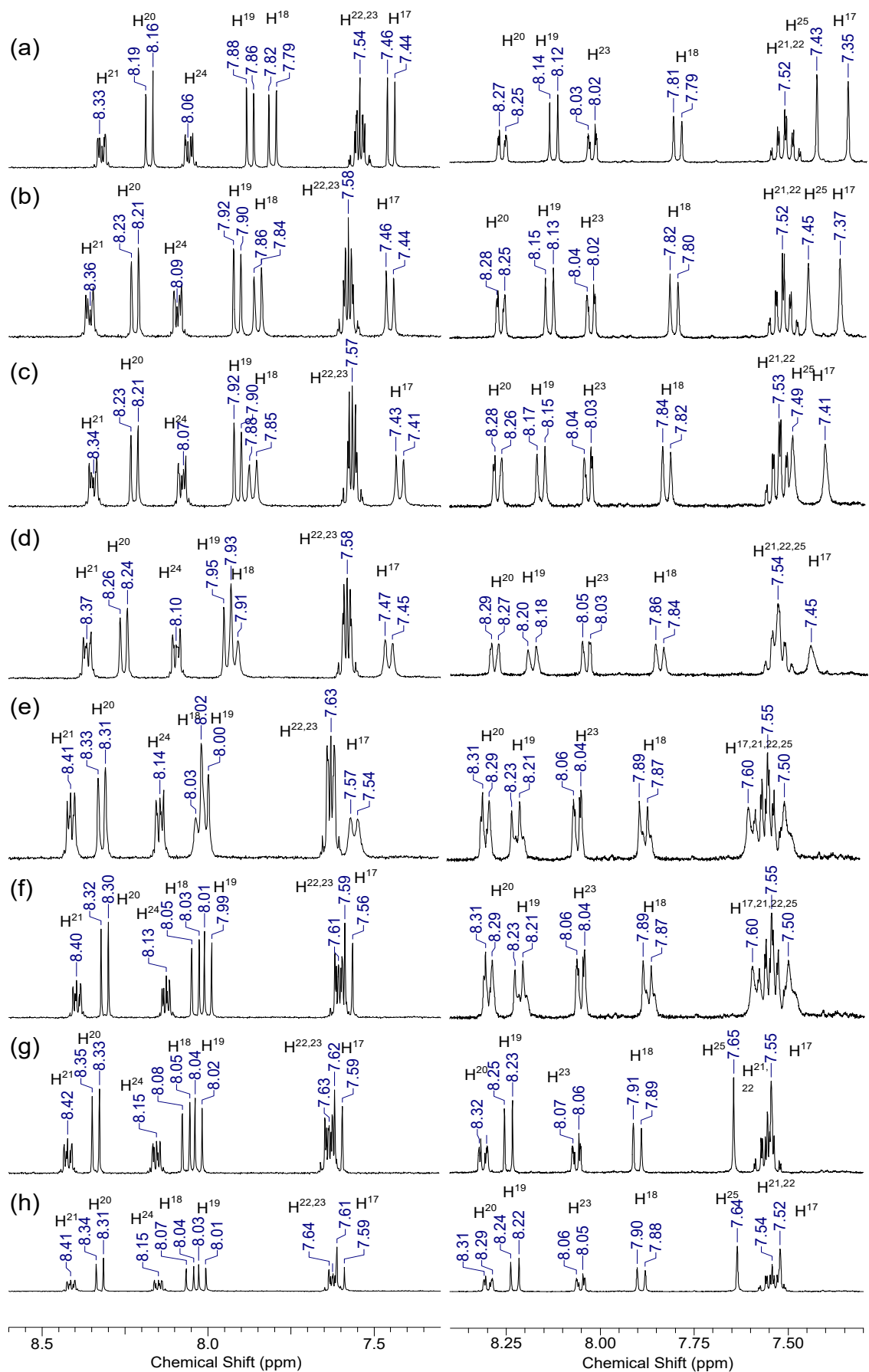


**Figure S17** NMR titration (400 MHz, CD<sub>3</sub>CN) results of **1** (left) and **2** (right) Ba(ClO<sub>4</sub>)<sub>2</sub> (aromatic part). Salt to crown ether ratio: (a) - 0; (b) - 0.1; (c) - 0.3; (d) - 0.5; (e) - 0.7; (f) - 1; (g) - 1.5; (h) - excess.

#### 4.2. UV-Vis and fluorescence titration

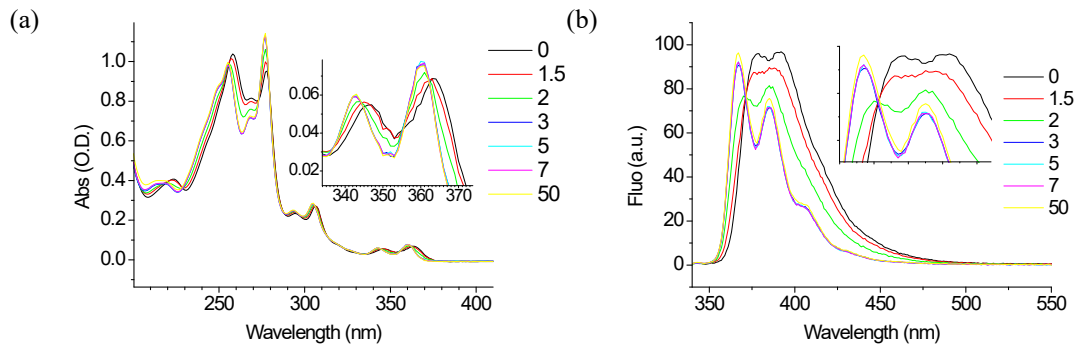


**Figure S18.** Absorbtion (a) ( $\text{CH}_3\text{CN}, 2 \times 10^{-5}\text{M}$ ) and fluorescence (b) ( $(\text{CH}_3\text{CN}, 2 \times 10^{-5}\text{M}, \lambda_{\text{ex}} = 305 \text{ nm})$ ) spectra of **1** upon the addition of  $\text{Ba}(\text{ClO}_4)_2$ . Added equivalents of the salt is shown in the legend.

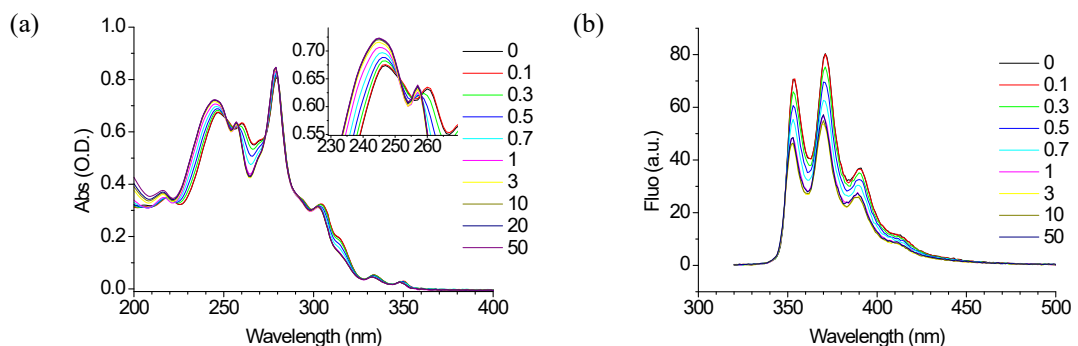


**Figure S19.** Absorbtion (a) ( $\text{CH}_3\text{CN}, 2 \times 10^{-5}\text{M}$ ) and fluorescence (b) ( $(\text{CH}_3\text{CN}, 2 \times 10^{-5}\text{M}, \lambda_{\text{ex}} = 310 \text{ nm})$ ) spectra of **2** upon the addition of  $\text{Ba}(\text{ClO}_4)_2$ . Added equivalents of the salt is shown in the legend.

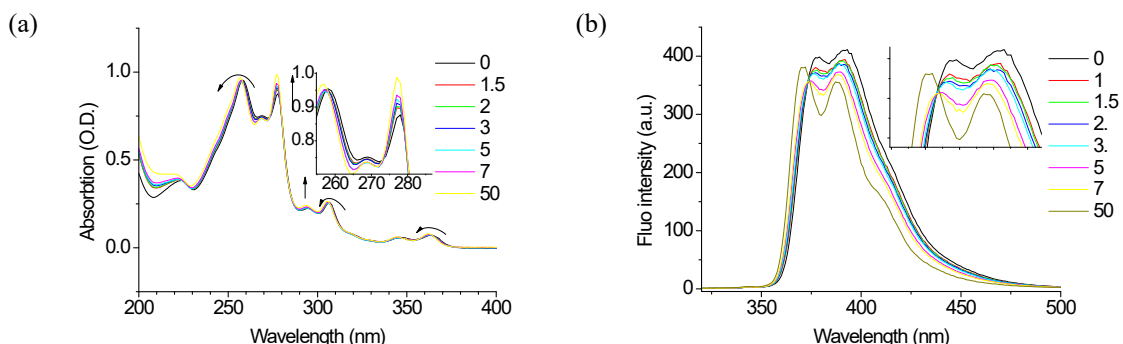


**Figure S20.** Absorbtion (a) ( $\text{CH}_3\text{CN}, 2 \times 10^{-5}\text{M}$ ) and fluorescence (b) ( $(\text{CH}_3\text{CN}, 2 \times 10^{-5}\text{M}, \lambda_{\text{ex}} = 305 \text{ nm})$ ) spectra of **1** upon the addition of NH<sub>4</sub>ClO<sub>4</sub>. Added equivalents of the salt is shown in the legend.

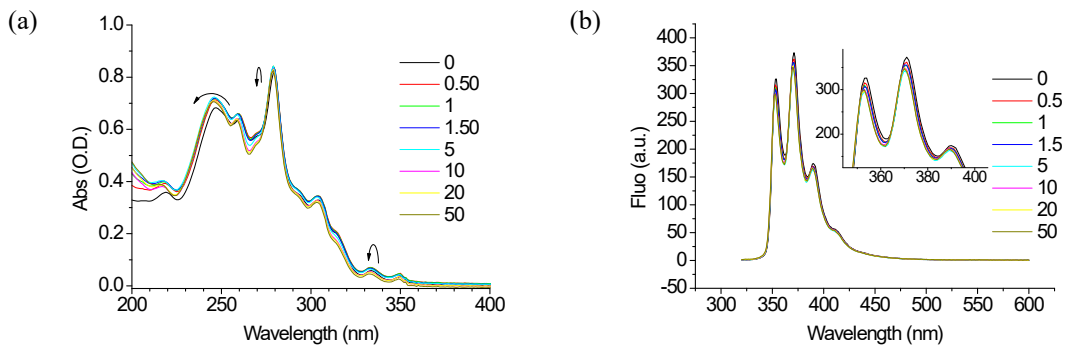


**Figure S21.** Absorbtion (a) ( $\text{CH}_3\text{CN}$ ,  $2 \times 10^{-5}\text{M}$ ) and fluorescence (b) ( $\text{CH}_3\text{CN}$ ,  $2 \times 10^{-5}\text{M}$ ,  $\lambda_{\text{ex}} = 310 \text{ nm}$ ) spectra of **2** upon the addition of  $\text{NH}_4\text{ClO}_4$ . Added equivalents of the salt is shown in the legend.

## 5. DOSY experiments on native and complexed CE 1 and CE 2.

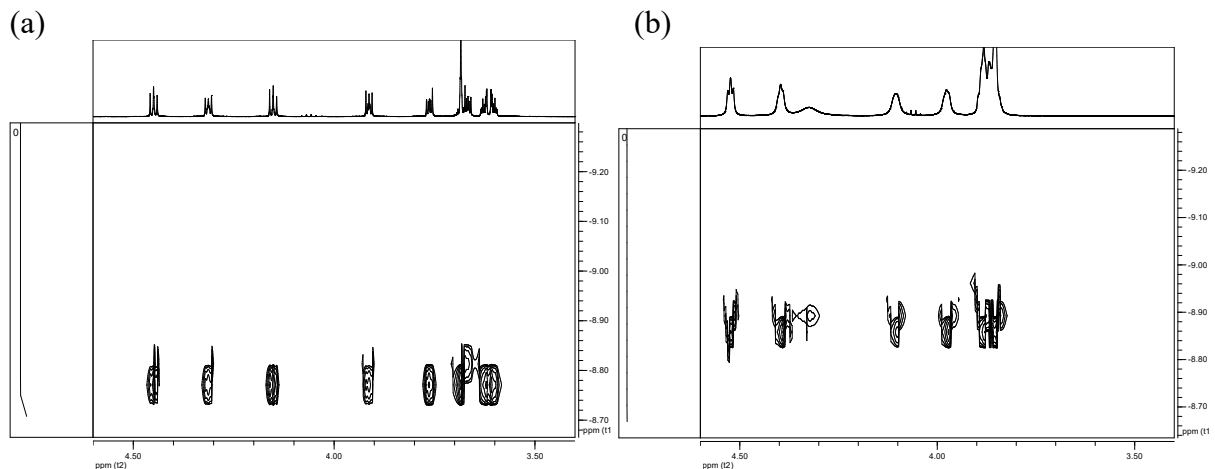


**Figure S22.** 2D DOSY experiments ( $0.011 \text{ M}$ ,  $\text{CD}_3\text{CN}$ , crown part is shown) of **CE 1** (a) free ligand; (b) in the presence of  $\text{Ba}(\text{ClO}_4)_2$  (**CE 1 : salt 1:1.2**). logD: **CE 1**: -8.8(at 3.92 ppm); **CE 2\*Ba}^{2+}** -8.9(at 4.10 ppm)

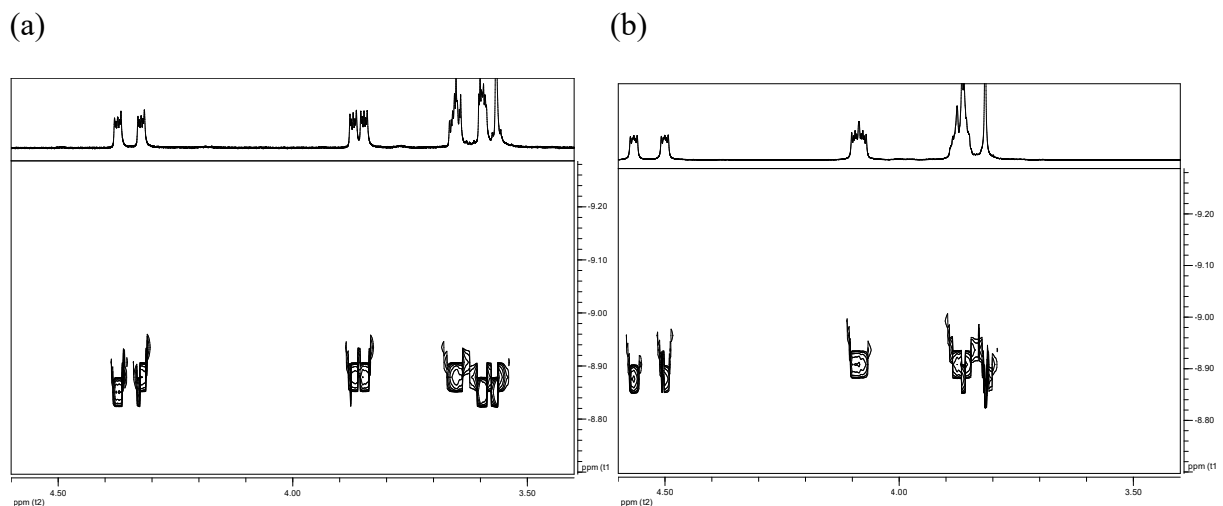


**Figure S23.** 2D DOSY experiments ( $0.012 \text{ M}$ ,  $\text{CD}_3\text{CN}$ , crown part is shown) of **CE 2** (a) free ligand; (b) in the presence of  $\text{Ba}(\text{ClO}_4)_2$  (**CE 2 : salt 1:1.2**) –logD: **CE 2**: -8.9(at 3.84 ppm); **CE 2\*Ba}^{2+}** -8.9(at 4.09 ppm)

## **6. Representative conformations of crown ethers 1 and 2.**

Energies of representative conformations of the isomers CE **1** and CE **2** were calculated using the methodology described in {Sharapa, 2019 #76}.

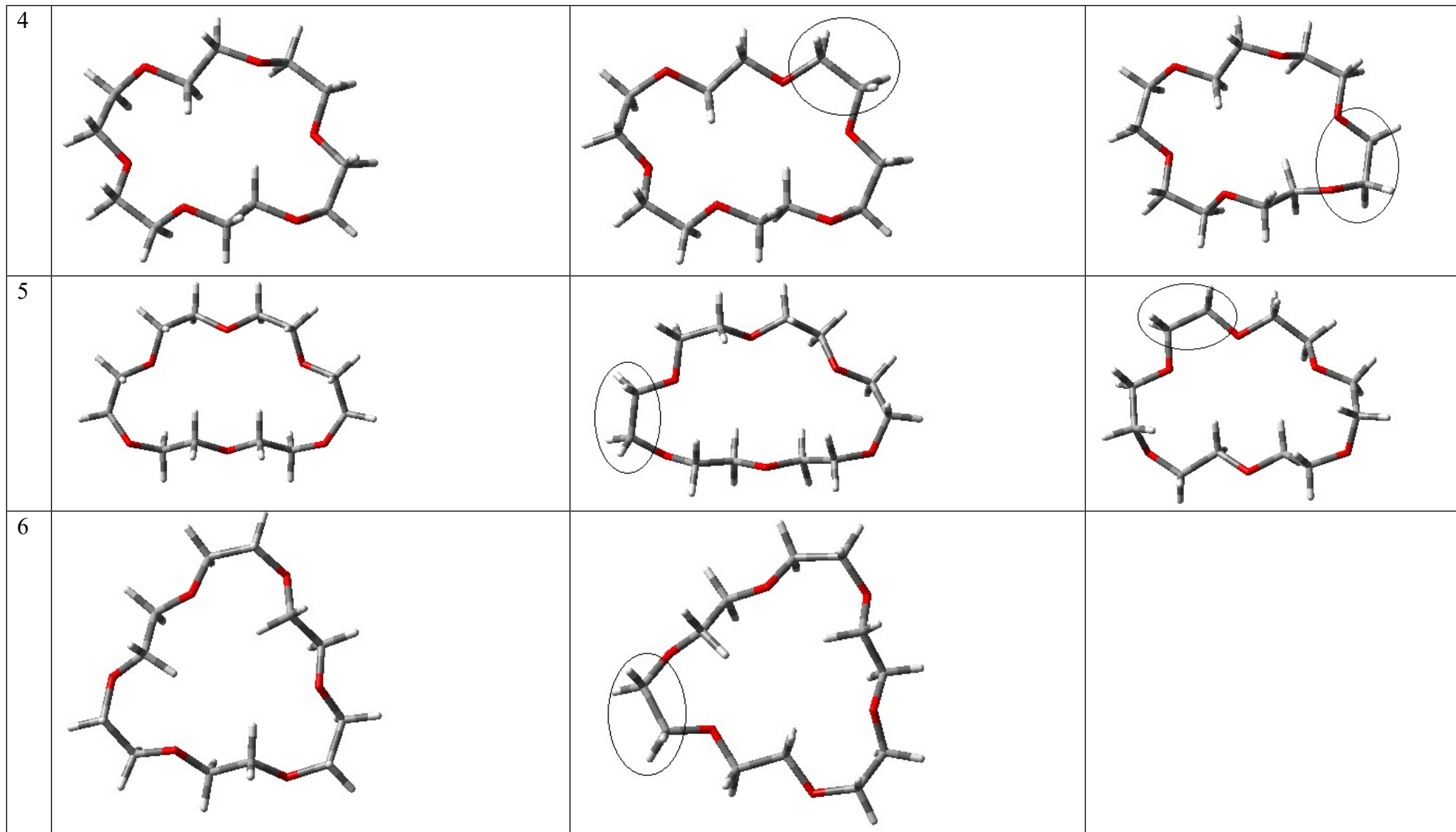
### **6.1. Generating conformations with dihedral angles close to 0 Deg**

First, optimized geometries from the Sullpementary info of {Sharapa, 2019 #76} were taken and fragments OCH<sub>2</sub>CH<sub>2</sub>O with dihedral angles *ca.* +/-60 Deg, unique from the symmetry viewpoint were determined. Then a relaxed potential energy surface scan has been peformed for the determined dihedrals driven from the starting angle to 0±5 Deg with 10 Deg increment. It was done to ensure that the part of the resulting conformations the non-influenced by this procedure to be as close to the starting ones as possible.

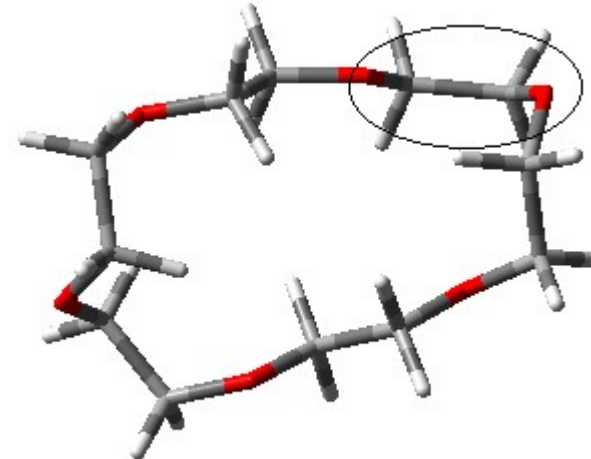
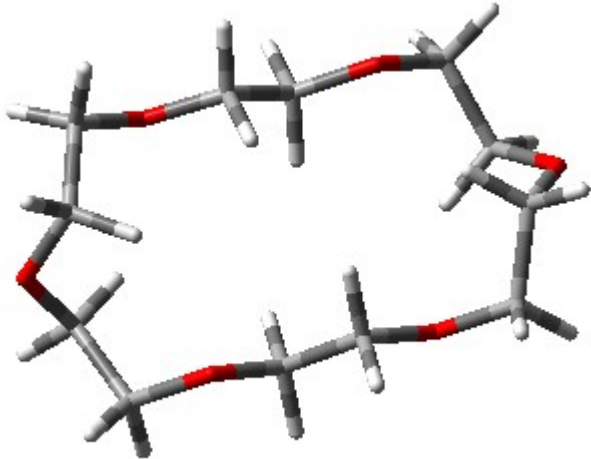
Also, a new conformation was generated from benzo-18-crown-6, in which a OCH<sub>2</sub>CH<sub>2</sub>O fragment closest to the benzo-ring is placed within the crown ether cavity (No.9).

**Table S1**

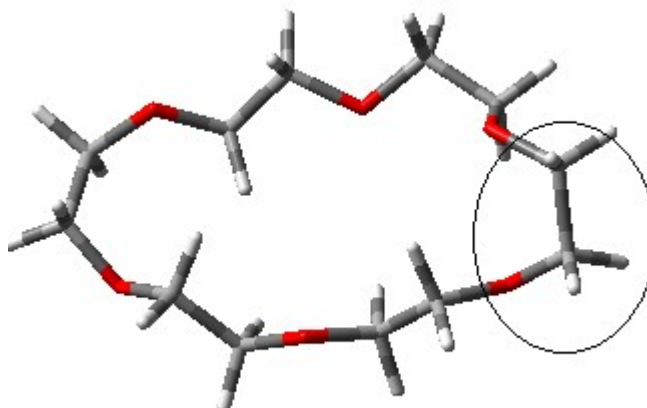
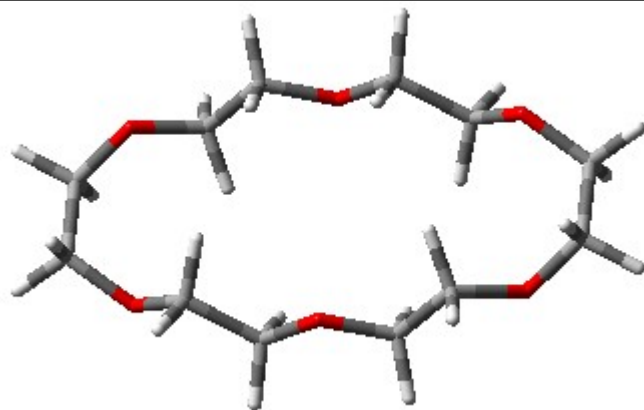
	Starting conformation	Conformation with a dihedral driven to <i>ca.</i> 0 Deg (the dihedral that was brought to <i>ca.</i> 0 is marked with the ellipse)	
1			
2			
3			



7



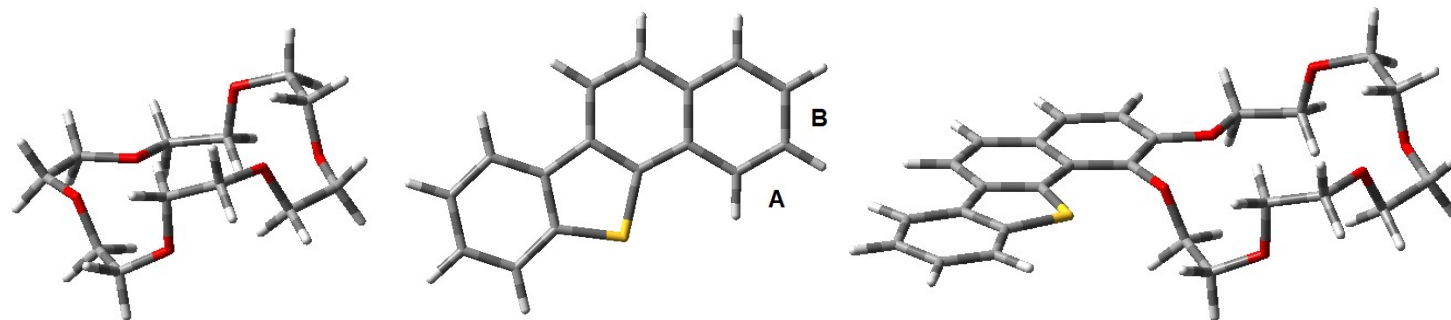
8



9\*

## **6.2. Docking of the aromatic fragment and MMF94 optimization both in vacuo and in $\text{CH}_3\text{CN}$ ( $\varepsilon = 38.8$ )**

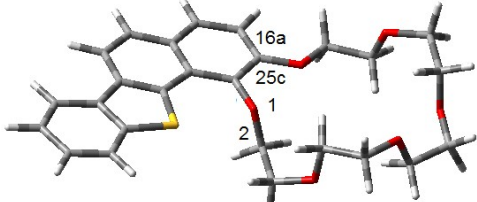
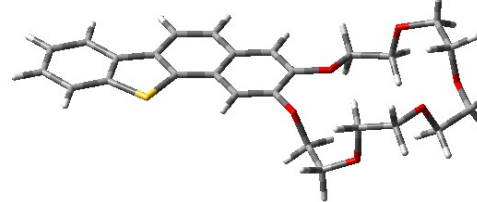
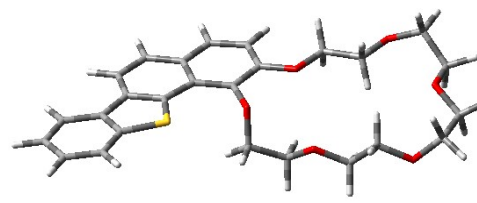
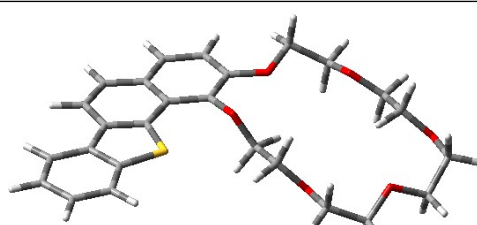
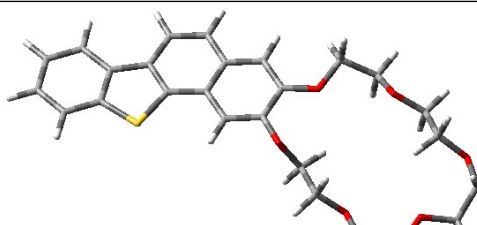
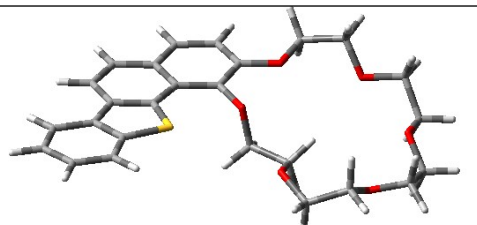
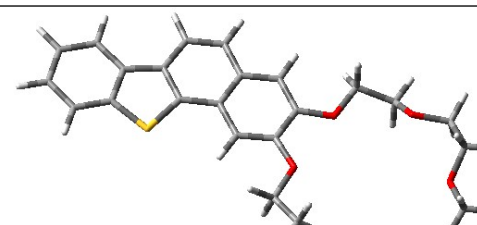
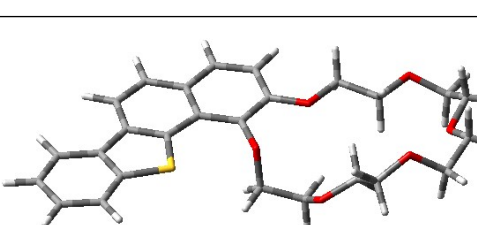
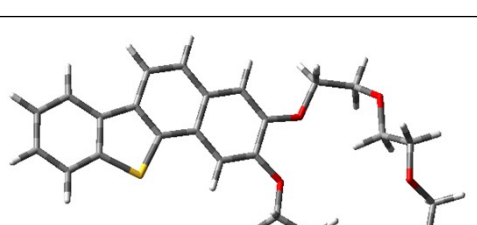
Obtained conformations of the 18-crown-6 with one dihedral angle close to 0 Deg was docked to different edges of the aromatic fragment to yield either CE **1** or CE **2** structure. Therefore, series of CE **1** and CE **2** conformations have been obtained, which were optimized by MM4 as realized in Chem 3D package. As the result, geometries of 12 conformations for each isomer was obtained, then, single point job at 6-31+g(d) level of theory was done to obtain the conformations' energies.

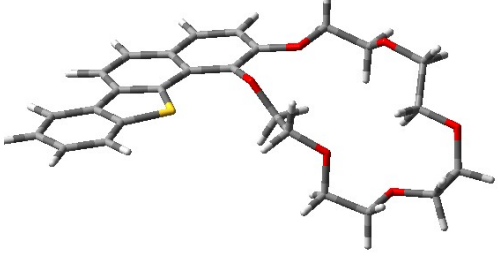
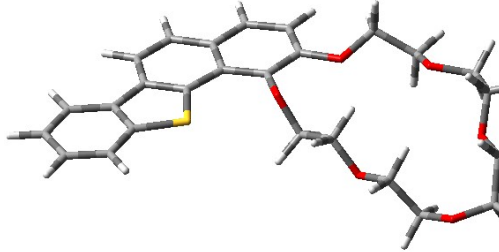
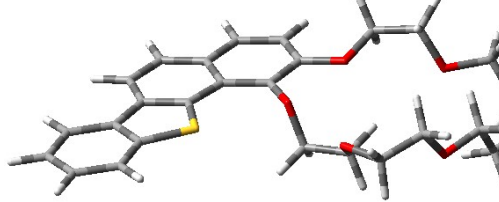
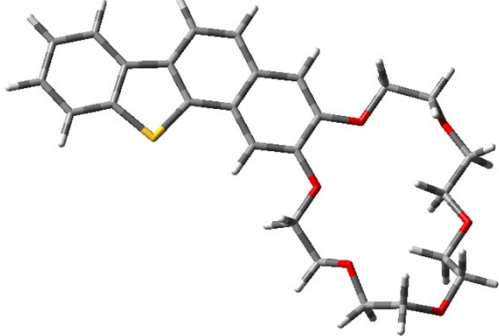
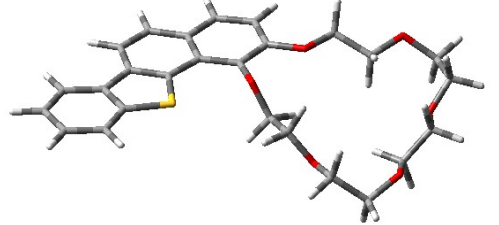
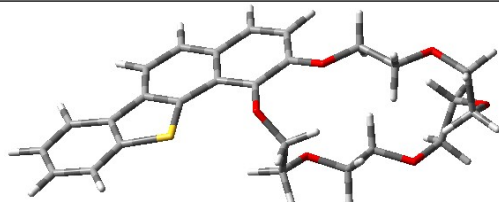
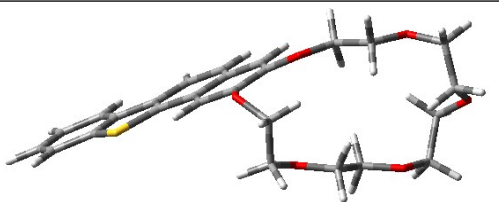
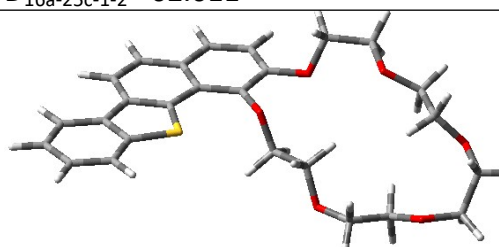
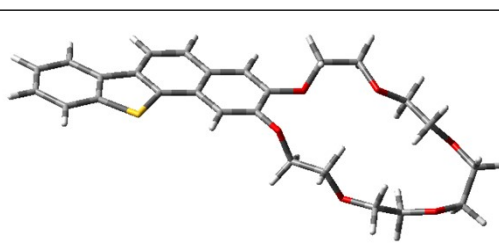


**Figure S24.** Example of docking of the dihedral-driven conformation 1 to the tetracyclic aromatic fragment to get the conformation of the CE **1**.

### 6.3. Single point energy and NMR chemical shifts calculations

**Table S2.** Crown ether conformations of CE **1** and CE **2** optimized by MMF94 force field.

CE 1 -c1		CE 2 -c1	
CE 1 -c2- 1		CE 2 -c2- 1	
CE 1 -c2- 2		CE 2 -c2- 2	
CE 1 -c3		CE 2 -c3	
CE 1 -c4- 1		CE 2 -c4- 1	

CE 1 -c4- 2		CE 2 -c4- 2	
	D <sub>16a-25c-1-2</sub> = -72.899		
CE 1 -c5- 1		CE 2 -c5- 1	
	D <sub>16a-25c-1-2</sub> = -71.395		
CE 1 -c5- 2		CE 2 -c5- 2	
	D <sub>16a-25c-1-2</sub> = 83.977		
CE 1 -c6		CE 2 -c6	
	D <sub>16a-25c-1-2</sub> = 74.675		
CE 1 -c7		CE 2 -c7	
	D <sub>16a-25c-1-2</sub> = 62.611		
CE 1 -c8		CE 2 -c8	
	D <sub>16a-25c-1-2</sub> = 81.024		

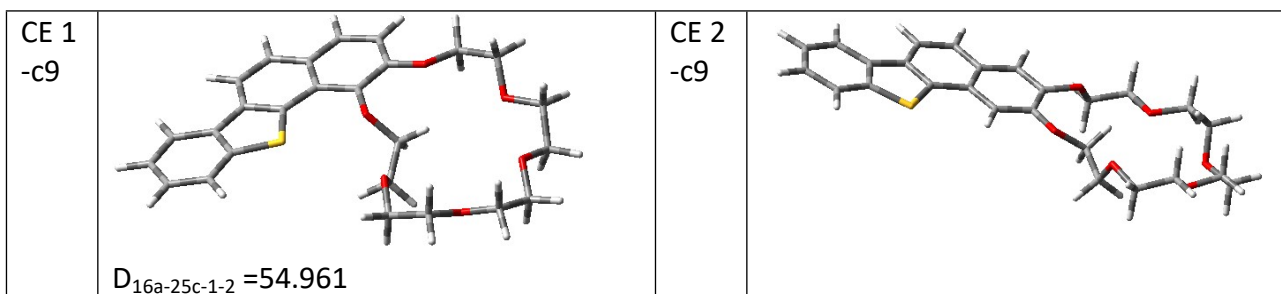


**Table S3** Energies of MMG94 optimized structures and their respective single point energies for sets of CE **1** and CE **2** conformations

CE <b>1</b>						CE <b>2</b>			
1	2	3	4	5	6	7	8	9	10
CE 1-c1	117.219	-1857.164865480	2.24	1.20%	-77.406	CE 2-c1	113.879	-1857.169739760	6.10
CE 1-c21	116.67	-1857.160432220	5.02	0.01%	-100.097	CE 2-c21	111.006	-1857.173981560	3.44
CE 1-c22	116.743	-1857.165271180	1.98	1.86%	-74.951	CE 2-c22	113.235	-1857.170460100	5.65
CE 1-c3	112.625	-1857.168135690	0.19	40.74%	-85.705	CE 2-c3	107.673	-1857.179456900	0.00
CE 1-c41	119.136	-1857.156639180	7.40	0.00%	-94.402	CE 2-c4-1	110.49	-1857.174125170	3.35
CE 1-c42	118.495	-1857.161645600	4.26	0.04%	-72.899	CE 2-c4-2	114.919	-1857.166938780	7.86
CE 1-c51	119.221	-1857.161676080	4.24	0.04%	-71.395	CE 2-c5-1	115.516	-1857.165911920	8.50
CE 1-c52	118.917	-1857.158585170	6.18	0.00%	-83.977	CE 2-c5-2	116.647	-1857.166099450	8.38
CE 1-c6	118.295	-1857.162092030	3.98	0.06%	-74.675	CE 2-c6	115.178	-1857.166234770	8.30
CE 1-c7	121.548	-1857.156939880	7.21	0.00%	-62.611	CE 2-c7	117.669	-1857.161376980	11.35
CE 1-c8	120.034	-1857.156030620	7.78	0.00%	-81.024	CE 2-c8	117.795	-1857.157485030	13.79
CE 1-c9	113.243	-1857.168431710	0.00	56.05%	-54.961	CE 2-c9	112.684	-1857.168431710	6.92
						Mean angle -67.93			

## 7. Facilitated ion transfer measurements

Voltammetric measurements were conducted by means of the amperometric ion-selective electrode (AISE), fig. S25. Plasticized membrane in a form of a conductive organic gel served as sensing element of the AISE. Organic membrane consisted of PVC (8 wt.%), *o*-NPOE as a plasticizer, 20 mM TClPhBTDA as an electrolyte of an organic phase, and crown-ethers **1** and **2** in various concentrations. To prepare the organic gel these components were mixed in a weighing flask at a temperature of 100–110 °C, then the mixture was left with stirring for 4–5 hours to full swelling of PVC. Heated to the molten state gel was applied to the front-end part of the electrode using dispenser, being left for 6 hours until completely solidified. To polarize the organic membrane and specify the potential, two electrodes are immersed into it: graphitic fiber, modified with ferrocene, as a reference electrode, and counter platinum electrode.

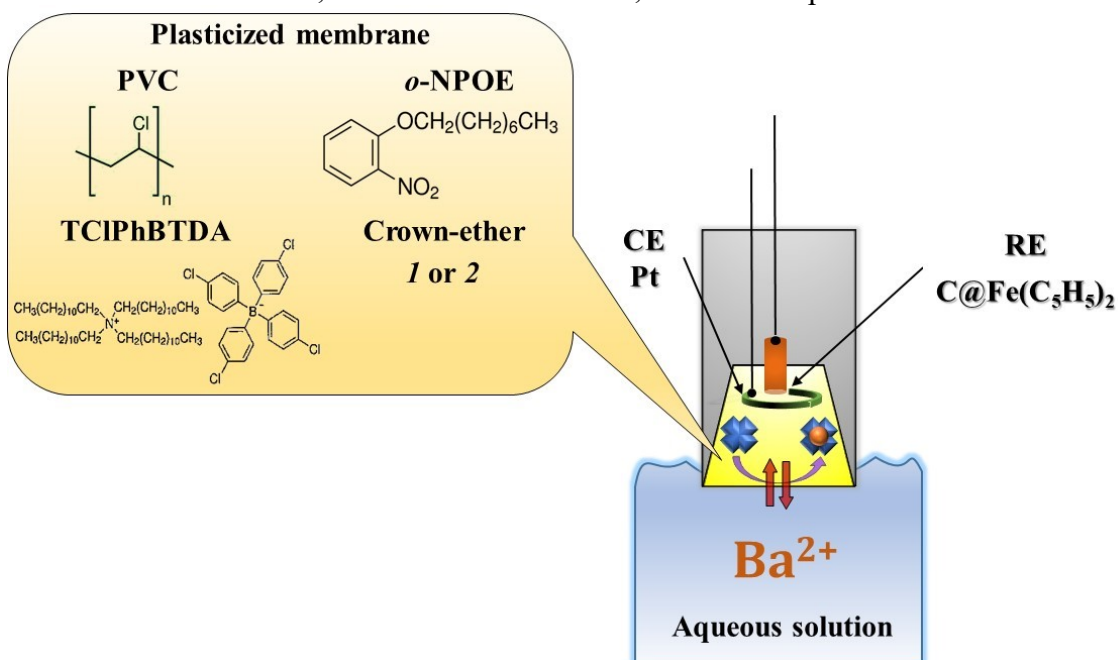


**Figure S25.** Schematic representation of the AISE with PVC-2-NPOE gel membrane used for voltammetric measurements of the interphase  $\text{Ba}^{2+}$  transfer: RE – reference electrode, CE – counter electrode.

Electrochemical measurements were performed by means of cyclic DC voltammetry using four electrodes. A 10 mM aqueous solution of LiCl was used as the supporting electrolyte in the aqueous phase. The reference electrode in the aqueous phase was a 3.5 M silver chloride electrode, the outer cavity was filled up with a 10 mM LiCl solution. The counter one was a platinum electrode. Electrochemical cell, employed for the studying of the process of complexation, is schematically represented in Fig. S26.

	Organic membrane:	Aqueous solution under study:		
$C_{\text{graphite}}$	$\text{Fe}(\text{C}_5\text{H}_5)_2$	$\text{o-NPOE}$ $\text{PVC (8 wt.\%)}$ $10^{-2} \text{ M TClPhBTDA,}$ $8\text{--}12 \text{ mM CE 1/2-12}$ $\text{mM CE 2}$	$10 \text{ mM LiCl} + x \text{ M } \text{Ba}^{2+}$	$10 \text{ mM LiCl}$ $\text{AgCl, 3.5 M KCl}$ $\text{Ag}$

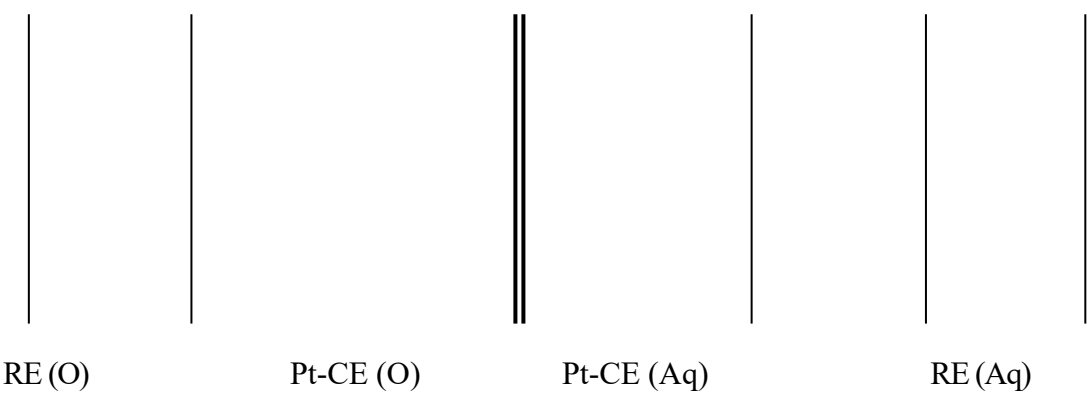


**Figure S26.** Chart of PCV-2-NPOE membrane based amperometric ion-selective electrode for voltamperometric measurements of  $\text{Ba}^{2+}$  phase-transfer. (RE – reference electrode; CE – counter electrode)